

Article

Bifurcation Control on the Un-Linearizable Dynamic System via Washout Filters

Chi Zhai ^{1,2}, Chunxi Yang ¹ and Jing Na ^{1,*}

¹ Faculty of Mechanical and Electrical Engineering, Kunming University of Science and Technology, Kunming 650093, China

² Faculty of Chemical Engineering, Kunming University of Science and Technology, Kunming 650500, China

* Correspondence: najing25@163.com

Abstract: Information fusion integrates aspects of data and knowledge mostly on the basis that system information is accumulative/distributive, but a subtle case emerges for a system with bifurcations, which is always un-linearizable and exacerbates information acquisition and presents a control problem. In this paper, the problem of an un-linearizable system related to system observation and control is addressed, and Andronov–Hopf bifurcation is taken as a typical example of an un-linearizable system and detailed. Firstly, the properties of a linear/linearized system is upon commented. Then, nonlinear degeneracy for the normal form of Andronov–Hopf bifurcation is analyzed, and it is deduced that the cubic terms are an integral part of the system. Afterwards, the theoretical study on feedback stabilization is conducted between the normal-form Andronov–Hopf bifurcation and its linearized counterpart, where stabilization using washout-filter-aided feedback is compared, and it is found that by synergistic controller design, the dual-conjugate-unstable eigenvalues can be stabilized by single stable washout filter. Finally, the high-dimensional ethanol fermentation model is taken as a case study to verify the proposed bifurcation control method.

Keywords: Andronov–Hopf bifurcation; washout filter; normal-form degeneracy; feedback stabilization



Citation: Zhai, C.; Yang, C.; Na, J. Bifurcation Control on the Un-Linearizable Dynamic System via Washout Filters. *Sensors* **2022**, *22*, 9334. <https://doi.org/10.3390/s22239334>

Academic Editors: Xue-Bo Jin and Yuan Gao

Received: 12 November 2022

Accepted: 27 November 2022

Published: 30 November 2022

Publisher's Note: MDPI stays neutral with regard to jurisdictional claims in published maps and institutional affiliations.



Copyright: © 2022 by the authors. Licensee MDPI, Basel, Switzerland. This article is an open access article distributed under the terms and conditions of the Creative Commons Attribution (CC BY) license (<https://creativecommons.org/licenses/by/4.0/>).

1. Introduction

In nonlinear systems covering ecology, economics, sociology and many other fields, complex dynamic evolutionary behaviors, such as multiplicity, self-oscillation, and even chaos arise in the vicinity of bifurcation points [1], and various methods are adopted to enhance sensory ability for accurate manipulation and control: the bifurcation oscillator is applied as a quantum state amplifier [2], the oscillating clearance of the rolling-element bear is taken as the bifurcating parameter with repetitive errors fused into the control system [3], and deep learning is implemented for the control of the Van del Pol system [4]. Mathematically, a bifurcation takes place at a parameter value where the system loses structural stability with respect to parameter variations, i.e., a phase portrait around the equilibrium is not locally topologically conjugate to the phase portraits around the equilibrium at nearby parameter values [5,6], which leads the solution manifold to change significantly, and exacerbates system information acquisition and control implementation [7,8].

Bifurcation control [9] refers to the task of designing a controller to suppress or reduce existing bifurcating dynamics, thereby achieving desirable dynamical behaviors, i.e., to obtain an asymptotically stable phase portrait. Feedback is often applied on a system with bifurcations, where the methods of linear/nonlinear feedback, washout-filter-aided feedback, impulse control, vibrational control, delayed feedback [10], etc., are frequently adopted. Nonlinear analysis and control based on harmonic balance approximations or nonlinear frequency response is also studied [11]. Recently, the idea of the anti-control of bifurcations [12] is proposed to segregate unwanted dynamics by deliberately introducing simple bifurcations into the system.

However, bifurcation control sometimes exhibits contradictory outcomes: improper control actions or process–model mismatch might cause the closed-loop system to move across the stable manifold, leading to more complicated dynamic behaviors [13], and one cause is that many control laws are developed on the basis of linear system theory (gain-scheduling, feedback linearization, etc.), but most dynamic systems with bifurcation are un-linearizable, i.e., truncating out the nonlinear terms alters the structural stability of the original system, and the higher-ordered-terms might not shrink to zero as the time approaches infinity. On the other hand, normal form degeneracy provides an effective way to evaluate those nonlinear terms, where types of bifurcations are expressed with quadratic or cubic degeneracy, and state-feedback based on normal forms and invariant sets are developed [14,15].

The main goal of this paper was to address the problem of an un-linearizable system in bifurcation control, where a comparative study is conducted on both the original and linearized models using washout-filter-aided state feedback. Through washout filters, a feedback signal is expected to be well geared with the open-loop dynamics and generate asymptotic outcomes. Abed and co-workers [16–19] implemented washout filters for bifurcation control, and feedback stabilization theory is proposed through auxiliary state variables that are inter-coupled. For systems with varying bifurcation parameters, the adaptive control scheme is also developed [12]. Since washout-aided feedback is introduced to migrate out of unstable eigenvalues, Marquardt [20] suggested manipulating directly on the unstable eigenspace, and introducing a pair of complex conjugate eigenvalues instead. Zhang [21] further employed eigenvalue assignment to achieve bifurcation control with guaranteed transient dynamics. Chen [22] proposed a systematic way of choosing constants and control parameters for the control of a high-dimensional bifurcating system. However, for a complicated system, i.e., both single- and dual-unstable eigenvalues exist, and controller design could be rather sophisticated.

The aforementioned washout-filter-aided control was developed on the linearized system, and the linearization procedure might change the structural stability of the original system and cause redundant control actions. In this work, the elementary properties of a linearizable system are offered, which provides a comparison with the un-linearizable system when these properties fail. Then, the system under Andronov–Hopf bifurcation is taken as a typical case of an un-linearizable one and the related analysis and bifurcation control strategy are developed. Since washout-filter-aided control can migrate the unstable eigenvalues, numerical bifurcation analysis on the closed-loop system reveals that, by inserting only one washout filter to any of the dual-unstable eigenspaces, the system might be stabilized. Compared with previous developed control strategies [23], our method could downsize the numbers of washout filters, facilitating the application for more practical and general cases, especially for high-dimensional systems.

The inconsistency of feedback stabilization and numerical bifurcation analysis stems from the fact that many nonlinear systems with bifurcation are un-linearizable [24]. This work is organized as follows: Through the analysis of the normal form of Andronov–Hopf bifurcation, the properties of an un-linearizable system are detailed in this paper; then, washout-filter-aided feedback on the un-linearizable system is analyzed in contrast with previously developed washout-filter-aided control strategies; and the continuous ethanol fermentation model is taken as an example of the un-linearizable system and is discussed in detail, and finally, concluding remarks are provided last.

2. The Un-Linearizable System

2.1. Properties of the Linear System

Previously to the discussion on the nonlinear dynamic system, basic properties concerning the *linear system* are provided. Consider a system exhibiting outcomes (characters) M , and which is detected with finite numbers of sensible causes x_1, \dots, x_n , related by func-

tion f ; then, a linear/linearizable system starts as a weighted contribution of individual variables

$$M = f(x_1, x_2, \dots, x_n) \approx \frac{\partial f}{\partial x_1} x_1 + \frac{\partial f}{\partial x_2} x_2 \dots + \frac{\partial f}{\partial x_n} x_n. \quad (1)$$

Furthermore, the coupling relation between causes and outcomes is decoupled through variable substitution and combination, e.g., a 2×2 input–output system with a linearized form is given as follows,

$$M = \begin{bmatrix} M_1 \\ M_2 \end{bmatrix} = \begin{bmatrix} f_1(x_1, x_2) \\ f_1(x_1, x_2) \end{bmatrix} \approx \begin{bmatrix} \frac{\partial f_1}{\partial x_1} & \frac{\partial f_1}{\partial x_2} \\ \frac{\partial f_2}{\partial x_1} & \frac{\partial f_2}{\partial x_2} \end{bmatrix} \begin{bmatrix} x_1 \\ x_2 \end{bmatrix}. \quad (2)$$

Assume that the Jacobian matrix is non-singular, and a coordinate change $y = Ax$ exists that could diagonalize Equation (2)

$$\begin{bmatrix} M_1 \\ M_2 \end{bmatrix} \approx \begin{bmatrix} \frac{\partial f_1}{\partial x_1} & \frac{\partial f_1}{\partial x_2} \\ \frac{\partial f_2}{\partial x_1} & \frac{\partial f_2}{\partial x_2} \end{bmatrix} \begin{bmatrix} x_1 \\ x_2 \end{bmatrix} = A^{-1} \begin{bmatrix} J_{11} & 0 \\ 0 & J_{22} \end{bmatrix} A \begin{bmatrix} x_1 \\ x_2 \end{bmatrix} = A^{-1} \begin{bmatrix} J_{11}y_1 \\ J_{22}y_2 \end{bmatrix}, \quad (3)$$

where :

$$\begin{bmatrix} \frac{\partial f_1}{\partial x_1} & \frac{\partial f_1}{\partial x_2} \\ \frac{\partial f_2}{\partial x_1} & \frac{\partial f_2}{\partial x_2} \end{bmatrix} = A^{-1} \begin{bmatrix} J_{11} & 0 \\ 0 & J_{22} \end{bmatrix} A, \quad y = \begin{bmatrix} y_1 \\ y_2 \end{bmatrix} = A \begin{bmatrix} x_1 \\ x_2 \end{bmatrix}.$$

Equation (3) indicates that for a linear/linearizable system, outcomes can be departed as a sum of the weighted causes separately, and sets of causes can be found to correlate every outcome exclusively.

The above *linear system* properties are held for the linear-time-invariant (LTI) dynamic system. Given in state-space form, a multi-input–multi-output (MIMO) system undergoes Laplace transform and obtains similar distributive and decoupling properties

$$\begin{cases} x' = Ax + Bu + \zeta(x, u) \\ y = Cx + Du \end{cases} \xrightarrow{\text{Laplace}} \frac{y}{u} = G(s) \approx C \frac{B}{sI - A} + D, \quad (4)$$

where ζ is the nonlinear terms that are truncated out in the linearizable dynamic system, whilst y and u represent outcomes and causes, respectively.

Mention that many nonlinear controls are developed on the linearized system. In practical applications, the presence of system nonlinearities causes the dynamic behavior to be qualitatively different from one operating regime to another; hence, one might obtain linear (at a specific set-point) models valid within a “small” region about the linearization point, and perform local designs for a set of operating conditions and then construct a gain-scheduling scheme that interpolates controller gains as the process traverses the operating region.

Accordingly, un-linearizable dynamic systems are those truncating out ζ as it alters the structural stability of the original system, and many dynamic systems with bifurcation are un-linearizable. Since a system under Andronov–Hopf bifurcation has dual- unstable eigenvalues with planar phase portrait, which is a typical multivariate, un-linearizable case, the following analysis and control is focused on the systems with Andronov–Hopf bifurcation.

2.2. Normal Form Andronov–Hopf Bifurcation: A Typical Un-Linearizable System

A standard approach to study the behavior of ordinary differential equations (ODE) around a bifurcation point is through normal form analysis, which starts by center manifold degeneracy. For a parameterized dynamical system,

$$x' = f(x, a), \quad (5)$$

where $x \rightarrow f(x, \alpha) \in R^n$ and α is the bifurcation parameter, with equilibrium x_0 satisfying $f(x_0, 0) = 0$. Assume eigenvalues of the Jacobian about x_0 are $\lambda_{1,2} = \pm i\omega, \lambda_k < 0 (k = 3, 4, \dots, n)$, then, there exists $n-2$ invariant/center manifold that is tangent at the bifurcation point to the eigenspace of the neutrally stable eigenvalues $\lambda_{1,2}$. Specifically, for a small neighborhood of $\alpha \in (0, \delta)$ and within the invariant manifold exists a 2-dimensional attracting manifold and the coordinate change of the first two eigenspace; by introducing complex conjugates z and z^* , Equation (5) around x_0 can be given as

$$z' = i\omega z + g(z, z^*) \quad z \in C^1, \tag{6}$$

where $g(z, z^*)$ is the degenerated terms at $\alpha = 0$ and can be given explicitly through rules of implicit function theorem. Assume $S(z, z^*) \in R^{(n-2)}$ represents the stable manifold, the $n-2$ stable equivalence is provided as follows

$$\omega \left(z^* \frac{\partial S}{\partial z}(z, z^*) - z \frac{\partial S}{\partial z^*}(z, z^*) \right) = f_{3,\dots,n}(S(z, z^*), p(z, z^*)), \tag{7}$$

and the $n-2$ solutions are exponentially convergent to $S(t)$

$$x_{3,\dots,n}(t) = S(t) + O(e^{-\beta t}), \text{ as } t \rightarrow \infty, \tag{8}$$

where β is the positive convergent rate. Considering that $x_{3,\dots,n}$ are locally asymptotic and therefore can be neglected in a local stability analysis around the bifurcation point, in the following discussion, about the Andronov–Hopf bifurcation, a two-dimensional topologically equivalent eigenspace containing dual-unstable ($\lambda_{1,2} = \pm i\omega$) is discussed instead of Equation (5).

For a general two-dimensional parameterized system, i.e., $x = (x_1, x_2) \rightarrow f(x, \alpha) \in R^2, \alpha \in R$, linearization about the equilibrium gives

$$x' = A(\alpha)x + h(x, \alpha),$$

where :

$$A(\alpha) = \begin{pmatrix} a & b \\ c & d \end{pmatrix}, \tag{9}$$

where a, b, c and d are elements of the Jacobian $A(\alpha)$, which is simplified as A ; $h(x, \alpha)$ represents the higher-ordered term. The characteristic equation corresponding to A gives

$$\lambda^2 - \text{tr}(A)\lambda + \det(A) = 0$$

$$\Rightarrow \begin{cases} \lambda = \frac{1}{2}(\text{tr}(A) + \sqrt{\text{tr}(A)^2 - 4\det(A)}) \\ \lambda^* = \frac{1}{2}(\text{tr}(A) - \sqrt{\text{tr}(A)^2 - 4\det(A)}) \end{cases} , \tag{10}$$

where $\text{tr}(A)$ and $\det(A)$ are the trace and determinant, respectively. Andronov–Hopf bifurcation takes place at $\alpha = 0$ satisfying $\text{tr}(A) = 0$ and $\det(A) = \omega_0^2$. Assume in a small neighborhood $\alpha \in (0, \delta)$ that the eigenvalues are written as $\lambda_1(\alpha) = \mu + i\omega$ and $\lambda_2(\alpha) = \mu - i\omega$, where $\mu = \text{tr}(A)$ and $\omega^2 = \text{tr}(A)^2 - \det(A)$; then, $T(\alpha)$ exists to transform $A(\alpha)$ into canonical real form as follows

$$J = T(\alpha)A(\alpha)T^{-1}(\alpha) = \begin{pmatrix} \mu(\alpha) & -\omega(\alpha) \\ \omega(\alpha) & \mu(\alpha) \end{pmatrix}, \tag{11}$$

where $J^{-1} = J^T / (\mu^2 + \omega^2)$. Let $y = T(\alpha)x$ and Equation (9) turns to

$$\begin{cases} y_1' = \mu(\alpha)y_1 - \omega(\alpha)y_2 + o(|y|^2) \\ y_2' = \omega(\alpha)y_1 + \mu(\alpha)y_2 + o(|y|^2) \end{cases} . \tag{12}$$

Introducing $z = y_1 + iy_2$ and $z^* = y_1 - iy_2$ and Equation (12) presents one-dimensional equivalence as follows

$$z' = \lambda(\alpha)z + g(z, z^*), \quad (13)$$

with $g = o(z^2)$. Let $q(\alpha)$ be the eigenvector of λ_1 about $A(\alpha)$ and one can give an eigenvector $p(\alpha)$ corresponding to λ_2 . Since λ_1 and λ_2 are complex conjugates, p and q can be chosen so that the inner product satisfies $\langle q, p \rangle = 1$, and

$$\begin{aligned} \langle p, q^* \rangle &= \left\langle p, \frac{1}{\lambda_2} A q^* \right\rangle = \frac{1}{\lambda_2} \langle A^T p, q^* \rangle = \frac{\lambda_1}{\lambda_2} \langle p, q^* \rangle \\ &\Rightarrow \langle p, q^* \rangle = 0. \end{aligned} \quad (14)$$

Equation (11) after transposition has $T^T(\alpha)J^T = A^T(\alpha)T^T(\alpha)$, and if $p(\alpha)$ has the following form

$$p(\alpha) = \begin{pmatrix} p_1 \\ p_2 \end{pmatrix} = \begin{pmatrix} T_{11} - iT_{21} \\ T_{12} - iT_{22} \end{pmatrix}, \quad (15)$$

where T_{ij} is i -th line, j -th row element, then z has the explicit form as follows

$$z = \langle p(\alpha), x \rangle. \quad (16)$$

Considering $\langle q, p \rangle = 1$ and Equation (13), the original variable x has the only equivalent transform

$$x = \begin{pmatrix} q \\ q^* \end{pmatrix} (z \quad z^*). \quad (17)$$

Substituting Equation (17) into (16), one obtains

$$z' = \lambda(\alpha)z + \langle p(\alpha), F(zq + z^*q^*, \alpha) \rangle. \quad (18)$$

Here, the nonlinear term $F(x, \alpha)$ in Equation (9) after Taylor expansion gives

$$\begin{aligned} F(x, 0) &= \frac{1}{2}B(x, x) + \frac{1}{6}C(x, x, x) + O(\|x\|^4), \\ \text{with } \begin{cases} B_{1,2}(x, y) = \sum_{j,k=1}^2 \frac{\partial^2 F_{1,2}(\xi, 0)}{\partial \xi_j \partial \xi_k} \Big|_{\xi=0} x_j y_k \\ C_{1,2}(x, y, m) = \sum_{j,k=1,l=1}^2 \frac{\partial^3 F_{1,2}(\xi, 0)}{\partial \xi_j \partial \xi_k \partial \xi_m} \Big|_{\xi=0} x_j y_k m_l \end{cases}. \end{aligned} \quad (19)$$

Substituting Equation (19) into (18) and the second-order term B gives

$$z' = \lambda z + \frac{\langle p, B(q, q) \rangle}{2} z^2 + \langle p, B(q, q^*) \rangle z z^* + \frac{\langle p, B(q^*, q^*) \rangle}{2} z^{*2} + O(|z|^3). \quad (20)$$

Through a coordinate change in Equation (21) the second-order term vanishes and gives Equation (22)

$$z = \omega + \frac{\langle p, B(q, q) \rangle}{2\lambda} \omega^2 + \frac{\langle p, B(q, q^*) \rangle}{\lambda^*} \omega \omega^* + \frac{\langle p, B(q^*, q^*) \rangle}{2(2\lambda^* - \lambda)} \omega^{*2} \quad (21)$$

$$\omega' = \lambda \omega + O(|\omega|^3) \quad (22)$$

Similarly, the third-order term after coordinate change obtains

$$\begin{aligned} \omega' &= \lambda \omega + \sigma \omega^2 \omega^* + O(|\omega|^4), \\ \text{where :} \\ \sigma &= \frac{\langle p, C(q, q, q^*) \rangle}{2}. \end{aligned} \quad (23)$$

Next, let $\omega = \rho e^{i\phi}$ and Equation (23) turns to

$$\begin{cases} \rho' = \rho(\alpha - \rho^2) + \Phi(\rho, \varphi) \\ \varphi' = 1 + \Psi(\rho, \varphi) \end{cases}, \quad (24)$$

where :

$$\Phi = O(|\rho|^4); \quad \Psi = O(|\rho|^3).$$

Suppose that φ performs constant rate rotation and Equation (24) mapped to the rotating plane gives

$$\frac{d\rho}{d\varphi} = \frac{\rho(\alpha - \rho^2) + \Phi}{1 + \Psi} = \rho(\alpha - \rho^2) + (\rho, \varphi), \quad (25)$$

where :

$$R = O(|\rho|^4).$$

Assume that $\rho_0 = 0$ is the initial condition, solving Equation (24) that provides

$$\rho = e^{\alpha\varphi}\rho_0 + e^{\alpha\varphi}\frac{1 - e^{2\alpha\varphi}}{2\alpha}\rho_0^3 + O_1(|\rho_0|^4). \quad (26)$$

For a fixed $\alpha > 0$, there exists a limit cycle, and when $\varphi = 2\pi$, the state ρ_1 would turn back to the initial point

$$\rho_1 = e^{2\pi\alpha}\rho_0 - e^{2\pi\alpha}(2\pi + O(\alpha))\rho_0^3 + O_2(|\rho_0|^4). \quad (27)$$

Comparing Equations (26) and (27), it is found that the 4th- or higher-order terms are unaffected by the formation of limit cycles, and hence can be truncated out. Furthermore, an Andronov–Hopf bifurcation is structurally equivalent to the following standard form

$$\begin{pmatrix} \hat{x}'_1 \\ \hat{x}'_2 \end{pmatrix} = \begin{pmatrix} \alpha & -1 \\ 1 & \alpha \end{pmatrix} \begin{pmatrix} \hat{x}_1 \\ \hat{x}_2 \end{pmatrix} \pm (\hat{x}_1^2 + \hat{x}_2^2) \begin{pmatrix} \hat{x}_1 \\ \hat{x}_2 \end{pmatrix}. \quad (28)$$

As shown in the following schematic diagram, if Equation (28) is linearized by truncating out the nonlinear terms, the phase portrait shows that the outcome is asymptotically stable to the origin (Figure 1a); if the nonlinear terms at Equation (28) are preserved, the phase portraits of the Andronov–Hopf bifurcation would be super-critical (Figure 1b), where the periodic solution is stable, or sub-critical (Figure 1c), where the periodic solution is unstable, and the criterion for super- or sub-criticality is judged by the sign of the third-order term of Equation (28).

It is an obvious standard form of the Andronov–Hopf bifurcation system that differs from the linearized system as it either attracts or repels an oscillatory trajectory, while the linearized one exhibits a diverging trend in the whole phase portrait. Hence, the nonlinear terms in Equation (28) are indispensable, and a system with Andronov–Hopf bifurcation is un-linearizable.

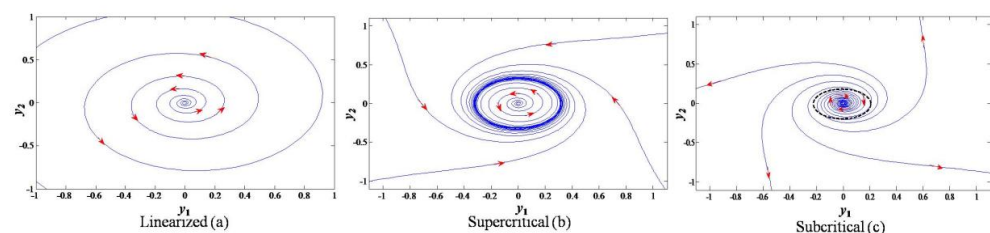


Figure 1. Phase portrait of (a) linearized system, (b) supercritical; and (c) subcritical Andronov–Hopf bifurcations, where $\alpha = 0.1$, and the arrows point out the time evolution direction.

Address that there exists two variables \hat{x}_1 and \hat{x}_2 interacting with one another to form a limit cycle around the Andronov–Hopf bifurcation point ($\alpha > 0$). Furthermore, Equation (28) can be represented one-dimensionally using complex variables, which means manipulating either \hat{x}_1 or \hat{x}_2 to affect the dynamic behavior of the system directly (or equally). Hence, introducing one state feedback suffices stabilizing a system with Andronov–Hopf bifurcation. Notion, the sign of the third-order term in Equation (28), decides whether the bifurcation is super-critical (–) or sub-critical (+), and one can refer to [21] for more details.

3. Stabilizing Normal Form Andronov–Hopf Bifurcation

3.1. Washout Filter as a State Manipulator

Since washout filters reject steady-state signals and passing transient ones, it could be used as a state manipulator and by fine-tuned feedback, eliminates the instabilities originating from open-loop bifurcations. Figure 2 is the washout-filter-aided controller design scheme: by inserting washout filters between states and outputs, transient dynamic behaviors are separated out that can be used to cancel out the perturbations of the system through feedback; while outputs preserve the steady state information, this is important for a control system, meaning washout filters are inoperative until vibrational signals are detected. Assume that x_k is the k -th element of the state variables, and d is the filter time constant. The control law used in this paper is quite simple, and v is the reference input used to determine the actual operating point and k is a controller parameter.

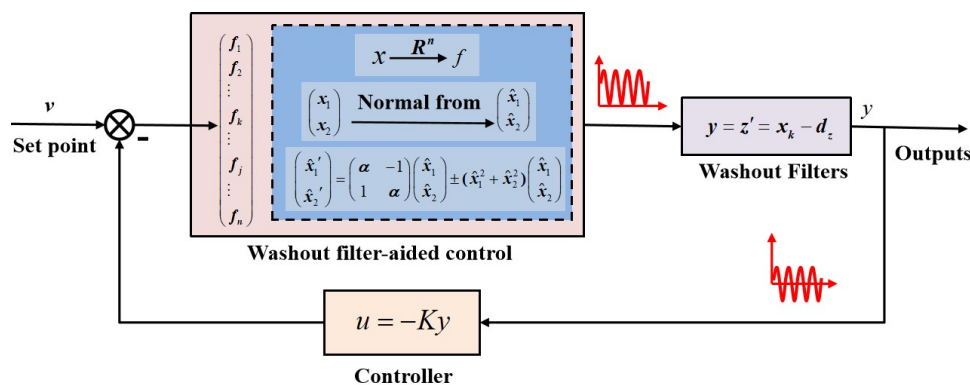


Figure 2. Block diagram for bifurcation control with washout-filter-aided stabilization.

3.2. Feedback Stabilization Based on the Linearized System

To stabilize the normal-form Andronov–Hopf bifurcation, washout-filter-aided control is constructed. Without loss of generality, the linearized system is extended as follows

$$x' = Ax + Bu + h(x, u), \tag{29}$$

where the control $u = [u_1, u_2]^T$ takes $u = v + ky$, and k is the feedback gain; B is an arbitrary input-state transfer matrix and $h(x, u)$ represents the higher-ordered-terms.

Adding the auxiliary state satisfies $dz/dt = y$, and the closed-loop system is provided as follows

$$\begin{cases} x' = Ax + Bu + h(x, u) \\ z' = P(x - z) \\ u = K(x - z) \end{cases} . \tag{30}$$

Stabilizing Equation (30) requires the following augmented matrix A_C being Hurwitz

$$\begin{aligned} \begin{pmatrix} x' \\ z' \end{pmatrix} &= \begin{pmatrix} A + BK & -BK \\ P & -P \end{pmatrix} \begin{pmatrix} x \\ z \end{pmatrix} \\ &= A_C \begin{pmatrix} x \\ z \end{pmatrix}. \end{aligned} \quad (31)$$

Theorem 1. *If A is non-singular and (A, B) is stabilizable, there exists (P, k) , which makes A_C Hurwitz.*

Proof. A_C after similarity transforms of T_1 and T_2 gives

$$\begin{aligned} T_1 A_C T_1^{-1} &= \begin{pmatrix} I & 0 \\ 0 & P^{-1} \end{pmatrix} \begin{pmatrix} A + BK & -BK \\ P & -P \end{pmatrix} \begin{pmatrix} I & 0 \\ 0 & P^{-1} \end{pmatrix}^{-1} \\ &= \begin{pmatrix} A + BK & -KBP \\ I & -P \end{pmatrix}, \\ T_2 T_1 A_C T_1^{-1} T_2^{-1} &= \begin{pmatrix} I & M \\ 0 & I \end{pmatrix} \begin{pmatrix} A + BK & -BK \\ P & -P \end{pmatrix} \begin{pmatrix} I & M \\ 0 & I \end{pmatrix}^{-1} \\ &= \begin{pmatrix} A + BK + M & -AM - KBM - M^2 - KBP - MP \\ I & -M - P \end{pmatrix}. \end{aligned} \quad (32)$$

Through the following small gain analysis, the control (P, K) is obtained

$$\begin{aligned} AM + KBM + M^2 + KBP + MP &= 0, \\ \text{s.t.} \begin{cases} P = \varepsilon P_1 + O(\varepsilon^2) \\ M = M_0 + \varepsilon M_1 + O(\varepsilon^2) \end{cases}. \end{aligned} \quad (33)$$

Canceling the first- and second-order perturbational terms provides

$$\begin{cases} (A + BK + M_0)M_0 = 0 \\ (A + BK)M_1 + AP_1 = 0 \end{cases}, \quad (34)$$

where :

$$M_0 = -A - BK,$$

which dictates,

$$M_1 = -AP_1(A + BK)^{-1}. \quad (35)$$

Then, around M_0 in a small region, the only M satisfying Equation (33) is given

$$\begin{aligned} M &= M_0 + \varepsilon M_1 + O(\varepsilon^2) \\ &= -A - BK - \varepsilon AP_1(A + BK)^{-1} + O(\varepsilon^2) \end{aligned} \quad (36)$$

with A_C satisfying

$$T_2 T_1 A_C T_1^{-1} T_2^{-1} = \begin{pmatrix} -\varepsilon AP_1(A + BK)^{-1} + O(\varepsilon^2) & 0 \\ I & A_{C2}(2,2) \end{pmatrix}, \quad (37)$$

where :

$$A_{C2}(2,2) = A + BK + \varepsilon(AP_1(A + BK)^{-1} - P_1) + O(\varepsilon^2).$$

When (A, B) is stabilizable, $A + BK$ can be designed Hurwitz. Since A is non-singular, setting $P_1 = A^{-1}(A + BK)$, then $-\varepsilon AP_1(A + BK)^{-1}$ is Hurwitz, so as A_{C2} . Plus, proper feedback gain k can promise the good transient dynamics of the closed-loop system.

One can design P based on above perturbation theory, but how many washout filters needed to stabilize the system is still a problem, the following lemma provides some insights. \square

Lemma 1. *The parity of the unstable eigenvalues of $-P$ needs to be consistent with that of A to make A_C in Equation (31) be Hurwitz.*

Proof. From Equation (31), one has $\det(A_C) = \det(A)\det(-P)$; hence, $\text{sign}(\det(A_C)) = \text{sign}(\det(A)\det(-P))$. If all eigenvalues of A_C have a negative real part, then $\text{sign}(\det(A_C)) = (-1)^{2n}$, which leads to $\text{sign}(\det(A)\det(-P)) = (-1)^{n-l}(-1)^{n-r}$, where l represents the number of unstable eigenvalues of A , and r represents the corresponding numbers of $-P$, i.e., $l + r$ is an even number.

Therefore, to stabilize the normal form Andronov–Hopf bifurcation based on information of Equation (29), $-P$ needs to be a 2×2 matrix. The Laplace transform between state and control gives

$$\frac{u(s)}{x(s)} = K \frac{sI}{sI + P}. \tag{38}$$

Obviously, when the state $x(s)$ is one-dimensional, the washout filter has $d = P$, but for a multi-dimensional system, e.g., P is 2×2 , and the parameters of the washout filters are difficult to provide

$$\frac{sI}{sI + \varepsilon p^*} = \frac{s}{\Delta} \begin{pmatrix} s + \varepsilon p_{22}^* & -\varepsilon p_{12}^* \\ -\varepsilon p_{21}^* & s + \varepsilon p_{11}^* \end{pmatrix}, \tag{39}$$

where :

$$\Delta = s^2 + \varepsilon(p_{11}^* + p_{22}^*)s + \varepsilon^2(p_{11}^*p_{22}^* - p_{12}^*p_{21}^*).$$

In accordance with the form of washout filters, the higher-ordered terms in Equation (39) need to be simplified. Considering only the transient dynamics are concerned with washout filters, and based on the *Laplace extreme theorem*, s in Equation (39) takes maximal value, which leads to the idea of the form of washout filters

$$\frac{sI}{sI + \varepsilon P^*} = \begin{pmatrix} \frac{s}{s + \varepsilon(P_{11}^* + P_{22}^*)} & 0 \\ 0 & \frac{s}{s + \varepsilon(P_{11}^* + P_{22}^*)} \end{pmatrix}. \tag{40}$$

Meaning two washout filters with $d = \text{tr}(P)$ aid the controller design, and Equation (40) is decoupled. \square

3.3. Bifurcation Analysis on the Closed-Loop System

Consider only one washout filter is introduced to x_i with feedback $u = K_i y$, and (i, j) pairing generates four possible cases for a two-input–two-output system. The normal form Andronov–Hopf bifurcation is augmented and $h(x, u)$ explicitly presented

$$\begin{cases} x' = Ax + Bu + h(x, u) \\ z' = x_i - dz = y \end{cases} \Rightarrow \begin{cases} x' = \begin{pmatrix} a & -1 \\ 1 & a \end{pmatrix} \begin{pmatrix} x_1 \\ x_2 \end{pmatrix} - (x_1^2 + x_2^2) \begin{pmatrix} x_1 \\ x_2 \end{pmatrix} + K_i y \\ y' = f_i(x_i, K_i y) - dy \end{cases}, \tag{41}$$

where y is the washout-filter-output corresponding to x_i . Based on Routh–Hurwitz stability criterion [25], one can deduce the control gain K_i of the washout filter that stabilizes Equation (41), and the Jacobean of the augmented system gives

$$\tilde{A} = \begin{bmatrix} \begin{pmatrix} a & -1 \\ 1 & a \end{pmatrix} & (BK)_i \\ \frac{\partial f_i}{\partial x_1} \frac{\partial f_i}{\partial x_2} & (BK)_i - d \end{bmatrix}. \tag{42}$$

Expanding Equation (42) along the last column gives the characteristic polynomial P_c

$$\begin{aligned} P_c &= \det(\tilde{A} - \lambda I_{2+1}) \\ &= ((BK)_i - d - \lambda)(\lambda_{-i} - \lambda) + \left(\frac{\partial f_i}{\partial x_i}\right)_n \cdot (BK)_i(\lambda_{-i} - \lambda) \\ &= \left[((BK)_i - d - \lambda)(\lambda - \lambda_n) - \left(\frac{\partial f_i}{\partial x_1}\right)_n \cdot (BK)_i \right] (\lambda_{-i} - \lambda). \end{aligned} \quad (43)$$

One can design pairs of (K_i, d) to make eigenvalues of $[\sim]$ in Equation (43) stable, but λ_{-i} is kept unchanged. Meaning that, for the linearized system, dual-unstable eigenvalues need two washout filters.

However, Equation (41) is a nonlinear control, and the dynamics of f_i could be compensated through feedback. The Jacobian from Equation (42) ignores nonlinear correlations between system and control feedback, which leads to redundant control loops. When numerical bifurcation analysis is implemented, it is found that only one washout filter can stabilize the closed-loop system represented by Equation (41).

One can design controllers through the identification of critical points for the emergence/elimination of unstable eigenvalues. For the case of Equation (41), the limit cycles when $\alpha > 0$ need to be eliminated (or stabilized); hence, with the aid of a washout filter framed in Figure 2, Andronov–Hopf bifurcation points in the (K_i, d) domain can be located numerically (refer to Appendix A for more details).

Substantial configurations are provided in Figure 3, where the solid lines are Andronov–Hopf bifurcation curves. BT represents Bogdanov–Takens bifurcation, and ZH represents zero–Hopf bifurcation, both of which are codimension-2 bifurcations originating from Andronov–Hopf bifurcation curves. Since x_1 and x_2 in Equation (41) are somewhat symmetric, configurations C1 and C4 are identical, and so are C2 and C3. For each stabilizable region, $d > 0$ implies the analog signal after washout filters are stable, while $d < 0$ means that the feedback signal is unstable.

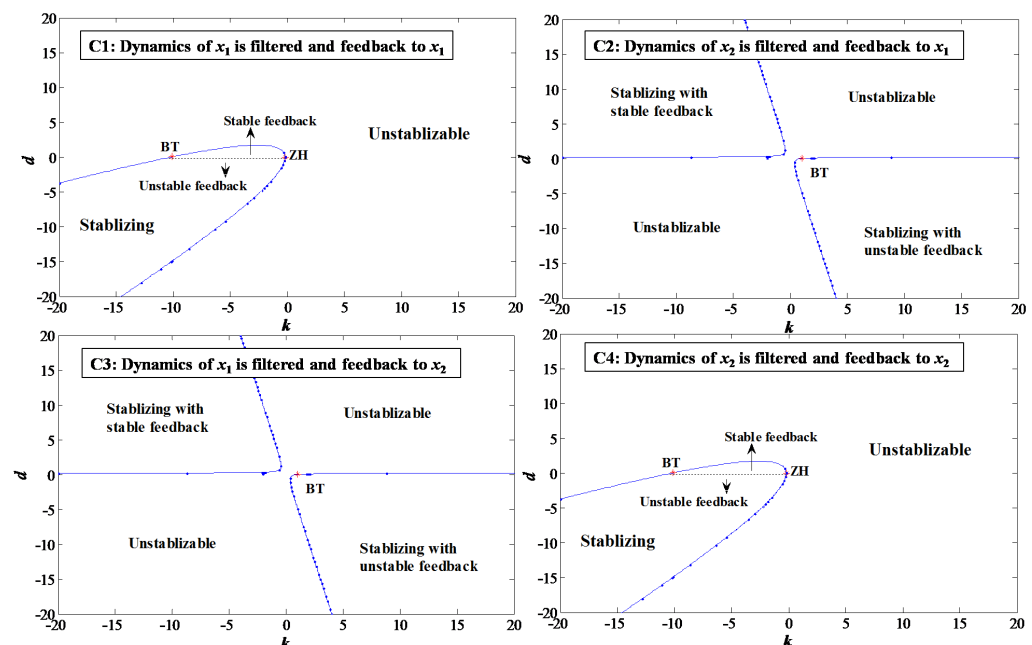


Figure 3. Analysis on the closed system of normal form Andronov–Hopf bifurcation.

As shown in Figure 3, the Andronov–Hopf bifurcation curves separate out parameter space (K_i, d) that stabilizes the closed-loop system. Mention $d = 0$ in cases of C1 and C4 indicates that traditional PID control stabilizes the system. It is observed $d < 0$ is able to stabilize the system from a nonlinear analysis perspective, but the unstable washout

filter generates diverging signals which are dangerous for real-time applications where interference is unavoidable and is not recommended. Exclusively for $d > 0$, it is found **C2** and **C3** have broader stable margins than **C1** and **C4**, which implies manipulating variables and control feedback could be chosen such that stabilizing control is easy to achieve.

Based on an analysis in Figure 3, numerical simulations on the Simulink platform were conducted, where $\alpha = 0.1$ for Equation (41). As is shown in Figure 4, when the parameter pair $(-5, 0.5)$ is adopted for case **C1**, it is stabilizable. The perturbation output after washout filter damps down and so as the states x_1 and x_2 , and a positive phase shift between y and x_1 implies that the oscillatory dynamics of the control feedback and forward signal are well geared to stabilize the closed-loop system. Since x_1 and x_2 are coupled in the self-oscillatory system, stabilizing x_1 would cause x_2 to damp down. Further study of the information acquisition by the washout filter shows that, the stable one obtains oscillatory signals, while the unstable one is exponentially divergent, where the overall stable character of the closed-loop system is obtained by the subtraction of the forward and backward signals. Hence, to stabilize the self-oscillatory dynamic system, stable washout filters are suggested.

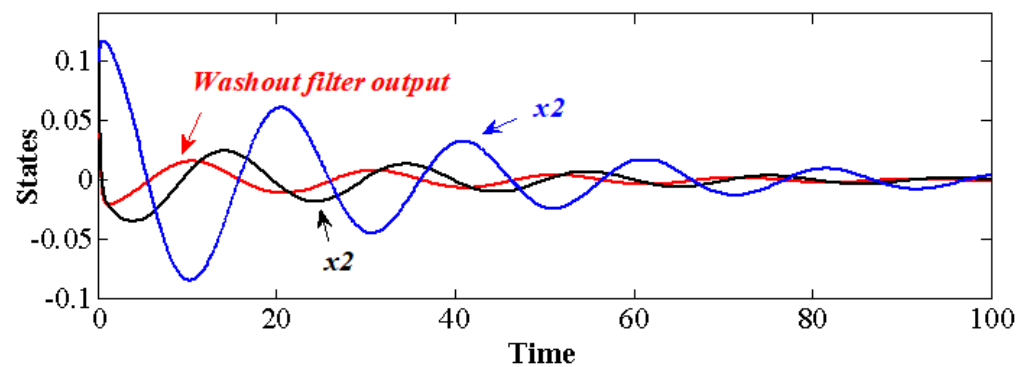


Figure 4. Time series of the closed-loop system, where the washout-filter-aided feedback parameters are $d = 0.5, k = -5$.

4. Case Study

4.1. Bifurcation Analysis on the Continuous Ethanol Fermentation Model

One of the most important bio-industrial sectors is the production of ethanol, which can be used as a gasoline additive to improve vehicle performance and reduce carbon emission. However, complex microorganism growth kinetics and ethanol inhibition present challenges for continuous production at the industrial scale, which limits the contribution of bio-fuel to current energy supply, and hence an exquisite controller design is critical to stabilizing the process. The structured model for *Zymomonasmobilis* fermentation [26] in a continuous stirred reactor is provided as follows, which considers the mass balance of the substrate (C_s , g/L), microorganism (C_x , g/L), K -compartment biomass (C_e , g/L), product (C_p , g/L) and the related parameters are given in Table 1

$$\begin{aligned}
 \frac{dC_s}{dt} &= \frac{\mu \cdot C_s \cdot C_e}{Y_{sx} \cdot (K_s + C_s)} - m_s \cdot C_x + D \cdot (C_{sf} - C_s) \\
 \frac{dC_x}{dt} &= \frac{\mu_{max} \cdot C_s \cdot C_e}{K_s + C_s} - DC_x \\
 \frac{dC_e}{dt} &= \frac{(k_1 - k_2 C_p + k_3 C_p^2) C_s \cdot C_e}{(K_s + C_s)} - DC_e \\
 \frac{dC_p}{dt} &= \frac{\mu_{max} \cdot C_s \cdot C_e}{Y_{px} \cdot (K_s + C_s)} + m_p \cdot C_x - DC_p
 \end{aligned} \quad (44)$$

where the dilution rate D and the substrate feed concentration C_{sf} are set as the design /operation parameters because of practical concerns. D is the reciprocal of the residence time

for the reaction stream, which has a fundamental impact on the bioreactor behavior; C_{sf} always comes from upstream, which may be interfered with due to upstream uncertainties.

Table 1. Parameters used for the continuous bio-ethanol reactor model.

Parameter	Definition	Value
μ_{max}	Maximum specific biomass growth rate (h^{-1})	1.0
Y_{sx}	Yield factor for substrate to biomass (g/g)	0.00244498
Y_{px}	Yield factor for substrate to product (g/g)	0.00526315
m_s	Maintenance substrate consumption rate (g/g h^{-1})	2.16
K_s	Monod constant (g/L)	0.5
k_1	Empirical constant (h^{-1})	16
k_2	Empirical constant (L/g h^{-1})	0.497
k_3	Empirical constant ($\text{L}^2/\text{g}^2\text{h}^{-1}$)	0.000383
m_p	Maintenance product consumption rate (g/g h^{-1})	1.1
C_{sf}	Substrate feed concentration (g/L)	140

With this model, nonlinear analysis is conducted on the open-loop system. A two-parameter bifurcation diagram decomposes the parameter space (D, C_{sf}) into different sections, and each has distinct dynamic properties. Furthermore, as is shown in Figure 5, the Andronov–Hopf bifurcation curve divides the parameter space into **S1** and **S2**. Any designing point at **S1** generates a self-sustained oscillator, while the point at **S2** is in stable steady equilibrium. Particularly, when C_{sf} is set as 140 g/L, **H** is detected at $D_H = 0.05024 \text{ h}^{-1}$. **H** is a supercritical Hopf bifurcation point due to its negative first Lyapunov coefficient (l_p), and operating the process with D at the left hand side of **H** leads to self-oscillations, while stable equilibriums are obtained on the right-hand side. It is obvious that the highest C_p is achieved when D is infinitesimal, which means that the reactor size needs to be very large. Since a high C_p of the bioreactor outlet cuts down the separation cost of later processing, one should design the reactor by setting D as the small reasonable equipment cost.

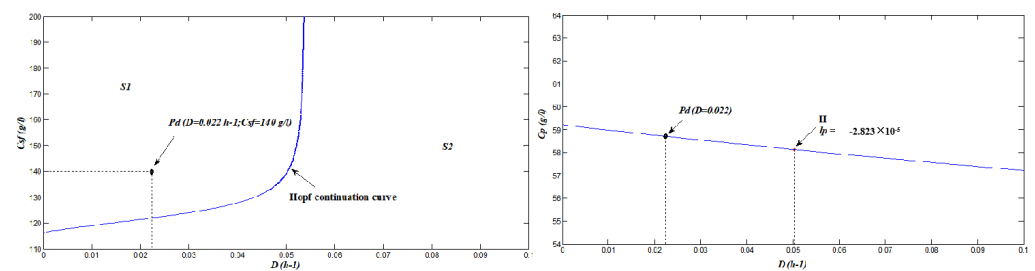


Figure 5. Bifurcation analyses on the ethanol fermentation process: two-parameter continuation diagram (left); and one-parameter continuation diagram (right).

We set the design point for Equation (44) as $P_d(0.022, 140)$ in this work, which falls into the self-oscillatory section. The idea of designing a self-oscillatory process was inspired by [27,28]. Taking P_d point as example, time average C_p is 8.8% higher than the corresponding steady-state output of the same design condition. However, the presence of self-oscillatory dynamics brings a challenge for the control of the continuous system; therefore, bifurcation control with the aid of washout filters is demanded to stabilize this multi-dimensional system.

4.2. Washout-Filter-Aided Control of the Fermentation Model

The model in Equation (44) is four-dimensional, and dual-unstable eigenvalues exist when Andronov–Hopf bifurcations emerge. For P_d , the equilibrium for C_s, C_x, C_e and C_p are 0.8509 g/L, 21.6547 g/L, 0.01915 g/L and 58.71 g/L, respectively; and the corresponding eigenvalues are $-2, -0.07136, 0.01232 \pm 0.1411$. Dual-unstable eigenspace emerges between

states C_e and C_p , indicating that the controlling variable would be chosen among them, C_p is set as the washout filter input, and it is assumed that C_p can be detected with online measuring devices. Then, the washout filter output is provided

$$\frac{y}{C_p} = \frac{s}{s+d} \Rightarrow y' = \frac{\mu_{max} \cdot C_s \cdot C_e}{Y_{px} \cdot (K_s + C_s)} + m_p \cdot C_x - DC_p - dy, \quad (45)$$

where d is the filter parameter, and to promise that y is stable and convergent, d needs to be positive. The manipulating variable is set to D , which is related to the input flow rate. Compared to the nominal $D_0 = 0.022 \text{ h}^{-1}$, the feedback by P control is provided

$$D = D_0 + ky, \quad (46)$$

where k is the feedback gain.

Combining Equations (44)–(46), one could implement bifurcation analysis on the closed-loop system. As is shown in Figure 6, when the washout-filter-aided P-control is facilitated on the continuous fermentation model, the controlling space (k, d) is separated into three sections by the Andronov–Hopf and neutral saddle curves, where only the upper-left one is stabilizable. Note that both Andronov–Hopf and neutral saddle bifurcations are codimension-1 bifurcations, and the bifurcations happening on these two curves are codimension-2 bifurcations. For the Andronov–Hopf bifurcation curve, three codimension-2 bifurcations, GH1 (0.1745, 0.0024), GH2 (0.0623, 0.0006) and ZH (0, 0.0005) are detected; and for the neutral saddle bifurcation curve, HH (0.02221, -0.03037) is detected. Mention for a given filter parameter, e.g., $d = 2$, with the decrease in k , that the dynamics of the closed-loop system evolves from stable to saddle, and then diverges.

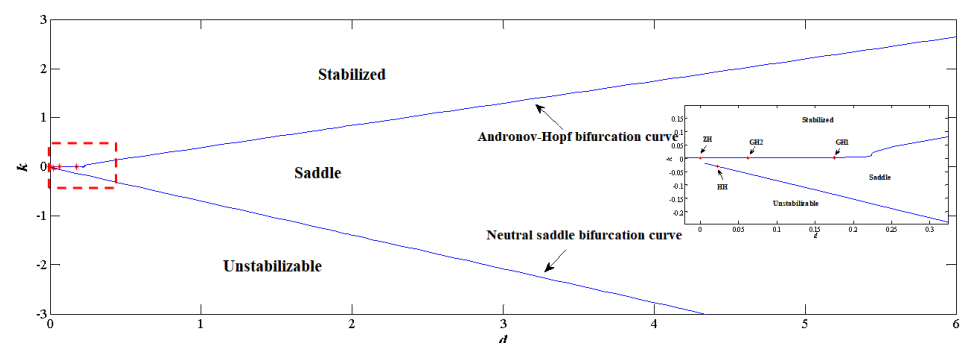


Figure 6. Two-parameter continuation diagram for the control variables, where GH1 and GH1 are the general Hopf bifurcation, ZH is the zero Hopf bifurcation and HH is the Hopf–Hopf bifurcation.

Further study is conducted by setting the control parameters to constant, e.g., $d = 2$ and $k = 1$, and observing the changes in the dynamics. As shown in Figure 7, between the two Andronov–Hopf bifurcation curves is the segment that can be stabilized by washout-filter-aided P-control. When the control is facilitated, stabilizing the designing point demands that C_p reaches the steady state, and then the washout filter output y has a tendency to converge towards zero, and Equation (45) tends towards zero; hence, the closed-loop system has the same equilibrium as the open-loop one, and $C_p = 58.71 \text{ g/L}$ is preserved at operational point P_d . As provided in Figure 8, the simulation results show converged dynamics after control $d = 2$ and $k = 1$, where C_p and D reach P_d as time approaches infinity.

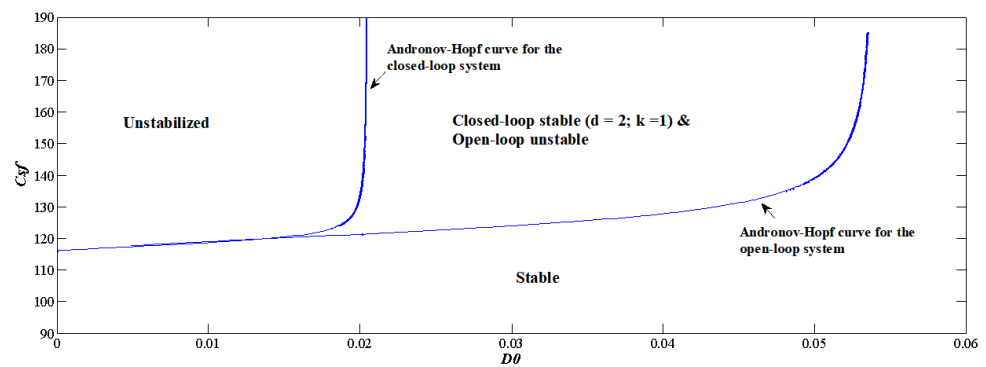


Figure 7. Two-parameter continuation diagram for the designing parameters.

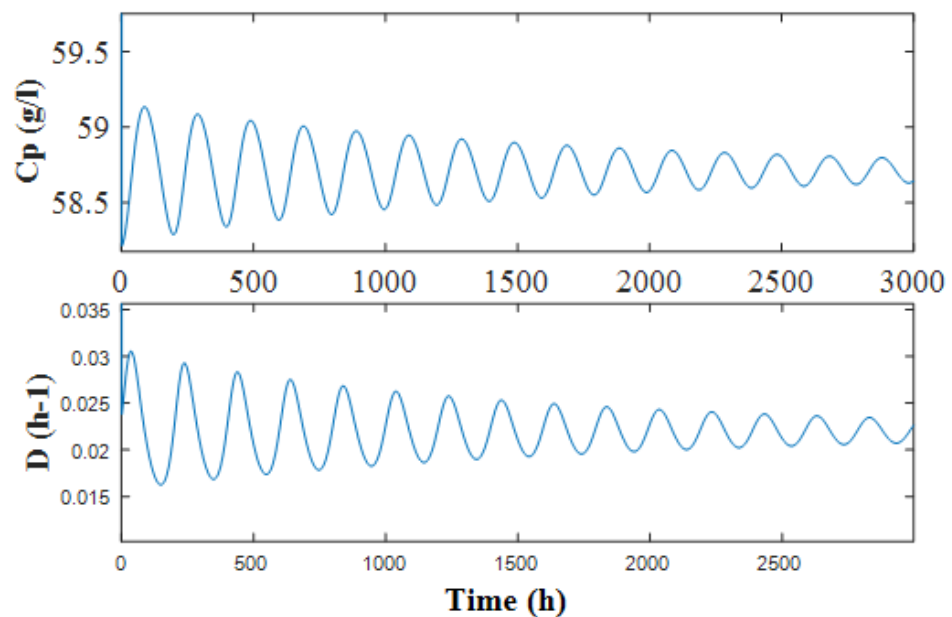


Figure 8. Stabilized outcomes for the closed-loop system, where $d = 2$ and $k = 1$.

5. Conclusions

In the presented study, we have focused on a subtle case with bifurcations, which is always un-linearizable and exacerbates information acquisition and a control problem. Taking the system with Andronov–Hopf bifurcation as a typical example, normal form analysis reveals that the cubic terms are the integral part of the whole system, and with the consideration of the un-linearizable characteristics, the stabilization procedure adopting washout-filter-aided control could realize the migration of dual-unstable eigenvalues with only one washout filter, which is not possible by previous control strategies. Moreover, the continuous ethanol fermentation process is taken as a case study for stabilizing a high-dimensional Andronov–Hopf bifurcation system: (1) variables mapping to the dual-unstable eigenspace are chosen as the manipulated variable; and (2) a stable washout filter parameter is demanded to stabilize the dual-unstable eigenvalues. By washout-filter-aided P-control, the ethanol fermentation process is stabilized and the equilibrium is preserved.

Author Contributions: All authors contributed to the study conception and design. Material preparation, data collection and analysis were performed by C.Z., C.Y. and J.N. The first draft of the manuscript was written by C.Z. and both authors commented on previous versions of the manuscript. All authors have read and agreed to the published version of the manuscript.

Funding: The authors gratefully acknowledge the National Natural Science Foundation of China–Yunnan basic research project (Grant No. 202001AU070048) for their support.

Data Availability Statement: All data generated or analyzed during this study are included in this published article.

Conflicts of Interest: The authors declare that they have no conflict of interest.

Nomenclature

D	dilution rate, h^{-1}
K_S	saturation constant, g/L
k_1, k_2, k_3	inhibition constant, L/g
T_0	inherent period, h
P_d	design point for unforced system
r_e	growth rate of the K-compartment, g/L h
C_{sf}	substrate feed concentration, g/L
t	time, h
x	biomass concentration, g/L
Y_{sx}, Y_{px}	yield factor of biomass on substrate/product, g/g
m_s	maintenance item, g/g h
<i>Greek letters</i>	
δ	Greek letters
μ_{max}	maximum specific growth rate, h^{-1}
<i>Subscripts</i>	
s	substrate
x	biomass
e	K-compartment
p	product

Appendix A

The following test function (Stephanos theorem) locates the critical points numerically. Stephanos theorem: If a $n \times n$ matrix A has eigenvalues $\mu_1, \mu_2, \dots, \mu_n$ ordered in an arbitrary order, then $2A \Theta I_n$ satisfies $(\mu_i + \mu_j)_{n > i > j} > 1$, and the function

$$\varphi_H(x, \alpha) = \det(2f_x(x, \alpha) \Theta I_n)$$

vanishes at an Andronov–Hopf bifurcation point, where “det” represents the determinant, and Θ is the bi-alternate product.

Proof. The eigenvalues of a matrix are preserved by similarity transforms as follows

$$(P \Theta P)(2A \Theta I_n)(P \Theta P)^{-1} = 2B \Theta I_n$$

where B is the transform of A , $B = PAP^{-1}$. Hence, one can assume that A is in upper triangular form (by reducing to the Jordan form if necessary). Then, the eigenvalues of A become its diagonal elements. By applying the equation below,

$$(2A \Theta I_n)_{(i,j)(k,l)} = \alpha_{ik} \begin{cases} -\alpha_{il} & \text{if } k = j \\ \alpha_{ik} & \text{if } k \neq i \text{ and } l = j \\ \alpha_{ii} + \alpha_{jj} & \text{if } k = i \text{ and } l = j \\ \alpha_{jl} & \text{if } k = i \text{ and } l \neq j \\ -\alpha_{jk} & \text{if } l = i \\ 0 & \text{else} \end{cases}$$

$2A \ominus I_n$ is an upper matrix if its indices are ordered lexicographically, and its diagonal elements are given as Stephanos theorem claims. By defining the test equation $\varphi_H(x, \alpha) = 0$, the critical point α_c can be located and inserted into the continuation sequence. \square

References

1. Wang, X.; Zhai, C.; Zhao, Z.; Palazoglu, A.; Sun, W.; Ai, J. Analysis of the Onset of Chaos for the Belousov-Zhabotinsky Reaction. *Comput. Aided Chem. Eng.* **2018**, *44*, 1375–1380.
2. Pashin, D.; Bastrakova, M.; Satanin, A.; Klenov, N.. Bifurcation Oscillator as an Advanced Sensor for Quantum State Control. *Sensors* **2022**, *22*, 6580. [[CrossRef](#)] [[PubMed](#)]
3. Ambrozkiewicz, B.; Syta, A.; Georgiadis, A.; Gassner, A.; Meier, N. Experimental Verification of the Impact of Radial Internal Clearance on a Bearing's Dynamics. *Sensors* **2022**, *22*, 6366. [[CrossRef](#)] [[PubMed](#)]
4. Zhai, H.; Sands, T. Comparison of Deep Learning and Deterministic Algorithms for Control Modeling. *Sensors* **2022**, *22*, 6362. [[CrossRef](#)] [[PubMed](#)]
5. Xu, C.; Liu, Z.; Liao, M.; Li, P.; Xiao, Q.; Yuan, S. Fractional-order bidirectional associate memory (BAM) neural networks with multiple delays: The case of Hopf bifurcation. *Math. Comput. Simul.* **2021**, *182*, 471–494. [[CrossRef](#)]
6. Yang, R.; Nie, C.; Jin, D. Spatiotemporal dynamics induced by nonlocal competition in a diffusive predator-prey system with habitat complexity. *Nonlinear Dyn.* **2022**, *110*, 879–900. [[CrossRef](#)]
7. Krishan, R.; Verma, A. Assessment and Enhancement of Hopf Bifurcation Stability Margin in Uncertain Power Systems. *Electr. Power Syst. Res.* **2022**, *206*, 107783. [[CrossRef](#)]
8. Alfifi, H.Y. Stability and Hopf bifurcation analysis for the diffusive delay logistic population model with spatially heterogeneous environment. *Appl. Math. Comput.* **2021**, *408*, 126362. [[CrossRef](#)]
9. Shi, J.; He, K.; Fang, H. Chaos, Hopf bifurcation and control of a fractional-order delay financial system. *Math. Comput. Simul.* **2022**, *194*, 348–364. [[CrossRef](#)]
10. Fiedler, B.; Flunkert, V.; Georgi, M.; Hövel, P.; Schöll, E. Refuting the odd-number limitation of time-delayed feedback control. *Phys. Rev. Lett.* **2007**, *98*, 114101. [[CrossRef](#)]
11. Zhai, C.; Sun, W. Analytical approximation of a self-oscillatory reaction system using the Laplace-Borel transform. *Chaos Solitons Fractals* **2021**, *142*, 110508. [[CrossRef](#)]
12. Cheng, Z. Anti-control of Hopf bifurcation for Chen's system through washout filters. *Neurocomputing* **2010**, *73*, 3139–3146. [[CrossRef](#)]
13. Hassouneh, M.A.; Lee, H.C.; Abed, E.H. Washout filters in feedback control: Benefits, limitations and extensions. In Proceedings of the 2004 American Control Conference, Boston, MA, USA, 30 June–2 July 2004; Volume 5, pp. 3950–3955.
14. Kang, W. Bifurcation control via state feedback for systems with a single uncontrollable mode. *SIAM J. Control. Optim.* **2000**, *38*, 1428–1452. [[CrossRef](#)]
15. Krener, A.J.; Kang, W.; Chang, D.E. Control bifurcations. *IEEE Trans. Autom. Control* **2004**, *49*, 1231–1246. [[CrossRef](#)]
16. Abed, E.H. A simple proof of stability on the center manifold for Hopf bifurcation. *SIAM Rev.* **1988**, *30*, 487–491. [[CrossRef](#)]
17. Abed, E.H.; Fu, J.H. Local feedback stabilization and bifurcation control, I. Hopf bifurcation. *Syst. Control Lett.* **1986**, *7*, 11–17. [[CrossRef](#)]
18. Abed, E.H.; Fu, J.H. Local feedback stabilization and bifurcation control, II. Stationary bifurcation. *Syst. Control Lett.* **1987**, *8*, 467–473. [[CrossRef](#)]
19. Abed, E.H.; Wang, H.O.; Chen, R.C. Stabilization of period doubling bifurcations and implications for control of chaos. *Phys. D Nonlinear Phenom.* **1994**, *8*, 154–164. [[CrossRef](#)]
20. Laiou, M.C.; Mönningmann, M.; Marquardt, W. Stabilization of nonlinear systems by bifurcation placement. *IFAC Proc. Vol.* **2004**, *37*, 675–680. [[CrossRef](#)]
21. Zhang, N.; Qiu, T.; Chen, B. Bifurcation control and eigenstructure assignment in continuous solution polymerization of vinyl acetate. *Chin. J. Chem. Eng.* **2015**, *23*, 1523–1529. [[CrossRef](#)]
22. Wang, H.; Zhang, N.; Qiu, T.; Zhao, J.; He, X.; Chen, B. Optimization of a continuous fermentation process producing 1,3-propane diol with Hopf singularity and unstable operating points as constraints. *Chem. Eng. Sci.* **2014**, *116*, 116. [[CrossRef](#)]
23. Ding, L.; Hou, C. Stabilizing control of Hopf bifurcation in the Hodgkin-Huxley model via washout filter with linear control term. *Nonlinear Dyn.* **2010**, *60*, 131–139. [[CrossRef](#)]
24. Suo, L.; Ren, J.; Zhao, Z.; Zhai, C. Study on the nonlinear dynamics of the continuous stirred tank reactors. *Processes* **2020**, *8*, 1436. [[CrossRef](#)]
25. Hurwitz, A. On the conditions under which an equation has only roots with negative real parts. *Math. Ann* **1895**, *46*, 273–284. [[CrossRef](#)]
26. Jobses, I.M.L.; Egberts, G.T.C.; Luyben, K.C.A.M.; Roels, J.A. Fermentation kinetics of *Zymomonas mobilis* at high ethanol concentrations: Oscillations in continuous cultures. *Biotechnol. Bioeng.* **1986**, *28*, 868–877. [[CrossRef](#)]
27. Douglas, J.M.; Rippin, D.W.T. Unsteady state process operation. *Chem. Eng. Sci.* **1966**, *21*, 305–315. [[CrossRef](#)]
28. Bailey, J.E. Periodic operation of chemical reactors: A review. *Chem. Eng. Commun.* **1974**, *1*, 111–124. [[CrossRef](#)]